Appl Phys B (2010) 100: 275–278
DOI 10.1007/s00340-010-3899-8

Applied Physics B
Lasers and Optics

Mid infrared interband cascade lasers for sensing applications

L. Nähle · P. Fuchs · M. Fischer · J. Koeth · A. Bauer · M. Dallner · F. Langer · S. Höfling · A. Forchel

Received: 7 October 2009 / Revised version: 16 December 2009 / Published online: 6 February 2010

Abstract The growth of Interband Cascade Laser material to cover the wavelength range from 3–4 µm is presented along with the fabrication and characterization of Broad Area (BA) and Ridge Waveguide (RWG) devices based on this material. Pulsed operation slightly below room temperature is observed for both device types, and a strong reduction of threshold currents can be observed in the RWG lasers. Variation of the active Quantum Well width in the epitaxial structures enables laser emission in the 3–4 µm wavelength region.

A growing demand for mid infrared (IR) light sources (wavelength ≈2.5–20 µm) is developing in several fields of application. Compact and reliable laser sources in this wavelength regime exhibit excellent possibilities of use for example in the military (e.g. detection of explosives [1]) and commercial (e.g. industrial process control [2]) sector, partially owing to naturally occurring atmospheric transparency windows.

The wavelength range from 3–4 µm is particularly interesting for several sensing applications, such as the detection of hydrocarbons. Existing types of semiconductor laser sources have closed in on this wavelength area [3, 4]. However, decreasing hole confinement and increasing Auger recombination in GaSb-based type I interband diodes limit their usability towards higher wavelengths of ≈4 µm. Intersubband quantum cascade lasers (QCL) approach the wavelength range mentioned from above but suffer from fast phonon scattering losses. From both issues of the above described laser types emerges the need of a more efficient laser source in the 3–4 µm regime.

The discussed issues can be circumvented by using interband cascade lasers (ICL) [5, 6]. These technologically demanding laser sources utilize optical transitions between an electron state in the conduction band and a hole state in the valence band in a cascade of Sb-based type-II QW structures. A broken-gap band edge alignment enables the tailoring of the emission wavelength by altering the cascade structures.

In this letter we report on a collaborative work between the University of Würzburg and nanoplus GmbH presenting broad area (BA) and ridge waveguide (RWG) lasers based on ICL epitaxial material. Each sample was grown in a solid-source molecular beam epitaxy chamber equipped with cracking cells for both arsenic and antimony and standard group-III effusion cells. A second indium cell as well as a dual dopant cell for silicon/galliumtelluride provided a convenient degree of flexibility during growth. Initially, an about 300 nm thick GaSb:Te buffering layer was grown on top of an epi-ready (100) GaSb substrate. The active region consisted of 6 to 12 active cascades (see Fig. 1) and was sandwiched in-between two 200 nm thick GaSb:Te separate confinement layers and 400 repetitions of a 2.4/2.3 nm InAs:Si/AlSb super lattice cladding. The cascade design was similar to the one described in [7] using a partly Si-doped chirped InAs/AlSb super lattice as injector and adjacent W-QWs as optically active part. Their thicknesses were varied from 1.85–2.5 nm in order to cover the 3–4 µm emission wavelength range. A highly doped InAs:Si capping layer finalized the structures and ensured low ohmic resistances.

L. Nähle (✉) · P. Fuchs · M. Fischer · J. Koeth
Nanoplus GmbH, Oberer Kirschberg 4, 97218 Gerbrunn, Germany
e-mail: lars.naehle@nanoplus.com
Fax: +49-931-9082719

A. Bauer · M. Dallner · F. Langer · S. Höfling · A. Forchel
Technische Physik, Universität Würzburg, Am Hubland, 97074 Würzburg, Germany

BA devices were fabricated using a broad stripe gold p-contact as etch mask. Applying reactive ion etching, the structures were etched well through the capping layer. A bottom contact was evaporated.

RWG devices were realized using a chromium etch mask. After deep ion etching below the active cascades the structures were passivated by a several hundred nanometers thick passivation layer before evaporating the top and bottom contact. The passivation was necessary in order to avoid surface leakage currents due to unterminated dangling bonds forming interfacial traps on the etched semiconductor surface [8]. The deep etching through the active layers was performed to confine the current path through the structure and avoid lateral leakage currents. An electron micrograph of the dry etched ridge with very smooth sidewalls along with the depiction of a cleaved facet of a finished RWG structure are shown in Fig. 2.

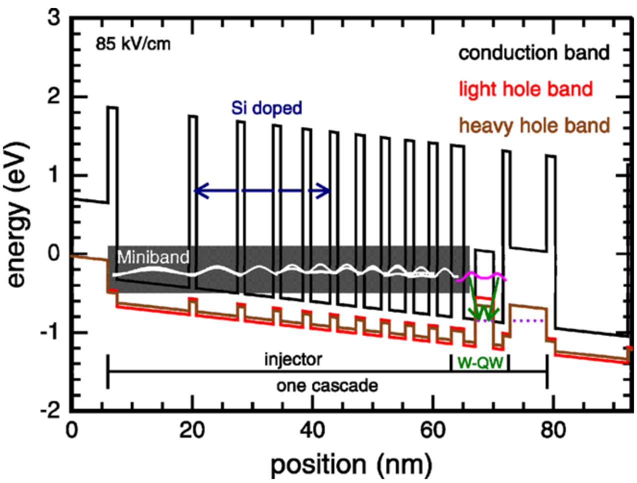

Fig. 1 Active cascade of the ICL structures used for the BA and RWG devices

Both BA and RWG devices were cleaved and mounted epi-side-up on copper heat sinks. Electro-optical characterization was conducted by installing the samples in a cryogenic cooler. Output power characteristics were investigated using a mercury cadmium telluride detector and spectral characteristics were studied employing an FTIR spectrometer. All measurements were conducted under pulsed conditions with 100 ns pulse width and 1 kHz repetition rate.

The results of these measurements for a BA device can be found in Fig. 3. P–I curves ranging from 100 to 290 K for a 2.0 mm × 0.1 mm device are shown on the left hand side. Threshold currents vary from 1.5 to 9.8 A at around room temperature. A representative U–I curve is integrated in the figure and shows an onset voltage of around 5.6 V. Spectral characterization shows coverage of the wavelength region

Fig. 2 Electron micrographs; *left*: dry etched ridge structure, *right*: cleaved facet of a RWG with passivation layers

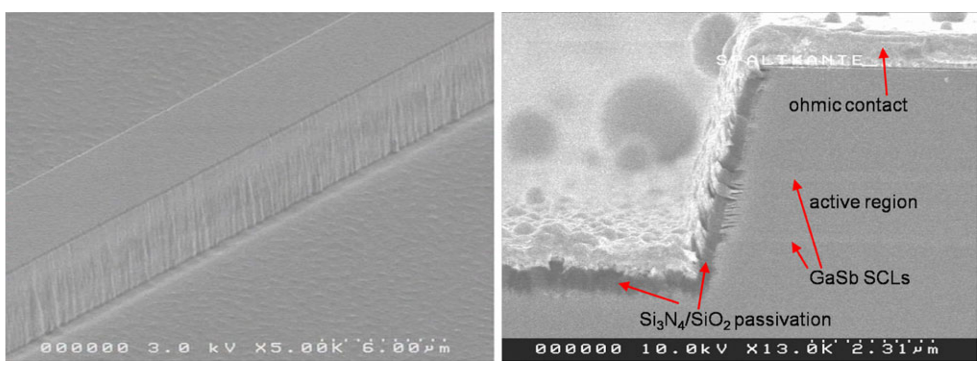

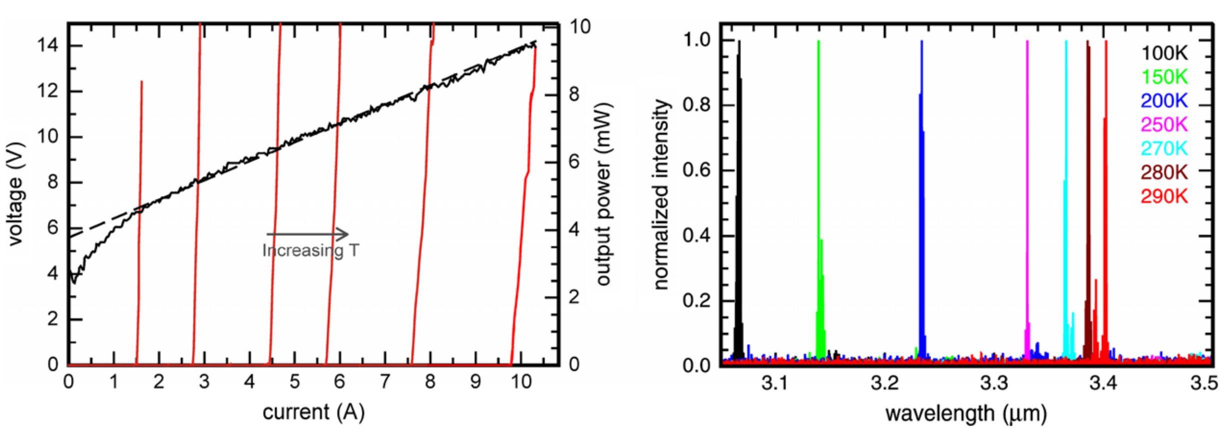

Fig. 3 Electro-optical characterization of a 2.0 mm × 0.1 mm BA device, *left*: P–I and U–I curves (U–I taken at 190 K), *right*: recorded spectra, both from 100–290 K

from 3.05 μm up to around 3.4 μm with varying temperature from 100 to 290 K. Selected spectra are presented on the right hand side of the graph.

In Fig. 4 results of comparative measurements on a 1 mm × 0.012 mm RWG structure can be observed. On the left hand side it can be clearly seen that the threshold currents of these devices are strongly reduced as compared to the BA devices, owing to the considerably smaller widths of the laser structures and the stronger confinement of the current path. Considering the temperature range from 100 to 280 K they vary from 0.15–0.72 A. Due to the smaller pumped laser volume the output powers are noticeably lower than in the BA devices. According to the U–I curve taken at 270 K the onset voltage in the RWG laser is slightly higher than in the BA laser, amounting to 6.0 V. This can most certainly be ascribed to a slightly better contacting of the BA lasers. Since the epitaxial structure is the same for both types of lasers the voltage drop along the active region should be the same in either case. On the right hand side of the figure the attained spectra for some selected temperatures are presented. They show basically the same behavior as in the BA devices. For comparison a wavenumber scale is included in the graph.

For both laser types the temperature shift of the gain of the ICL devices amounts to 1.7 nm/K or 1.7 cm^{-1}/K. The Fabry–Pérot mode spacing, which can be extracted

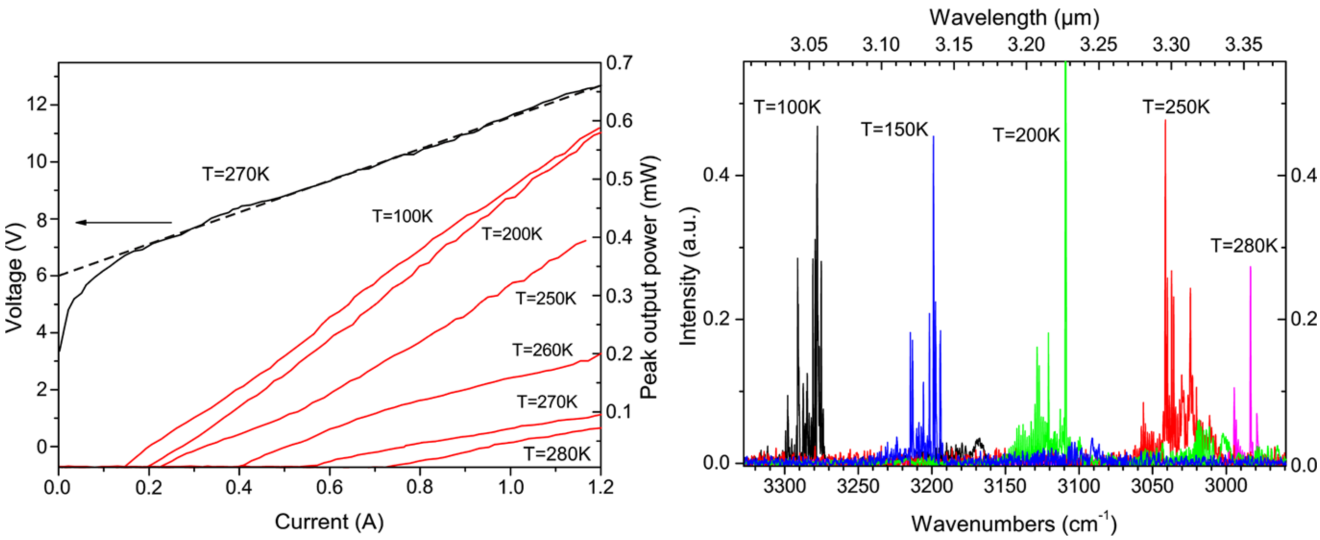

Fig. 4 Electro-optical characterization of a 1.0 mm × 0.012 mm RWG device, *left*: P–I and U–I curves, *right*: recorded spectra, both from 100–280 K

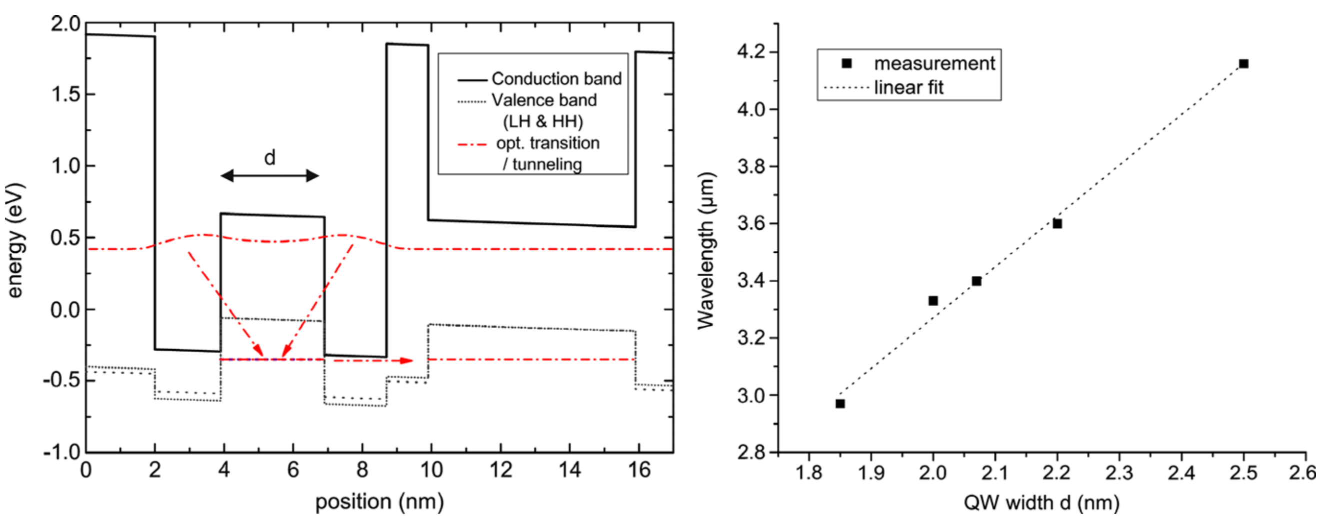

Fig. 5 *Left*: Depiction of a W-QW as used in the ICL active cascades along with the optical transition occurring. The QW width d was varied in order to attain an emission wavelength covering from 3 to 4 μm. *Right*: Measurement and fit of the emission wavelength of BA devices for a variation of the QW width

very accurately from the RWG measurements, is around $\Delta\lambda^{-1} = 1.7\ \mathrm{cm}^{-1}$, which yields a refractive group index of $n_{\mathrm{eff},g} = 3.65$, considering the 1 mm device length.

In order to cover the wavelength range from 3–4 μm different samples with varying QW widhts were grown. As depicted in Fig. 5, the width d of the active QW was varied from 1.85 to 2.5 nm. The emission wavelength at 77 K of BA devices manufactured on the different epitaxial materials is plotted against the QW width. The nearly linear dependence agrees very well with theoretical models that will be published elsewhere. The graph shows that, as intended, the wavelength range between 3 and 4 μm can be very well accessed using this approach.

Summarizing, the fabrication of BA and RWG lasers on ICL epitaxial material was presented along with characterization results for the two laser types. Both BA and RWG lasers operate up to slightly below room temperature and yield emission wavelengths varying from 3.05–3.4 μm with temperatures from 100–280/290 K. The threshold currents in the RWG devices are significantly reduced compared to the BA devices.

A study of the emission wavelength dependence on the variation of the active QW width in the active laser cascades showed very good results compared with theoretical models and enabled laser emission in the 3–4 μm wavelength region by tailoring the epitaxial structure.

References

1. C. Bauer, P. Geiser, J. Burgmeier, G. Holl, W. Schade, Appl. Phys. B **85**, 251 (2006)
2. M. Hümmer, K. Rößner, T. Lehnhardt, M. Müller, A. Forchel, R. Werner, M. Fischer, J. Koeth, Electron. Lett. **42**, 10 (2006)
3. L. Shterengas, G. Belenky, T. Hosoda, G. Kipshidze, S. Suchalkin, Appl. Phys. Lett. **93**, 011103 (2008)
4. S.Y. Zhang, D.G. Revin, J.W. Cockburn, K. Kennedy, A.B. Krysa, M. Hopkinson, Appl. Phys. Lett. **94**, 031106 (2009)
5. R.Q. Yang, Microelectron. J. **30**, 1043 (1999)
6. M. Kim, C.L. Canedy, W.W. Bewley, C.S. Kim, J.R. Lindle, J. Abell, I. Vurgaftman, J.R. Meyer, Appl. Phys. Lett. **92**, 191110 (2008)
7. C.L. Canedy, W.W. Bewley, J.R. Lindle, C.S. Kim, M. Kim, I. Vurgaftman, J.R. Meyer, Appl. Phys. Lett. **88**, 161103 (2006)
8. A. Gin, Y. Wei, J. Bae, A. Hood, J. Nah, M. Razeghi, Thin Solid Films **447–448**, 489 (2004)